
White Rose Research Online

eprints@whiterose.ac.uk
https://eprints.whiterose.ac.uk
Universities of Leeds, Sheffield and York

Deposited via The University of Leeds.

White Rose Research Online URL for this paper:
https://eprints.whiterose.ac.uk/id/eprint/220975/

Version: Accepted Version

Book Section:
Dutta, S. (2025) Adaptive Sliding Mode Controller Development to Improve Rail Network Efficiency through Virtual Coupling. In: Ravindra Kumar, V. M., K. P., Vineesh and Sharma, S.K., (eds.) Railway Engineering Technology: Developments and Innovations. CRC Press, Boca Raton, pp. 137-164. ISBN: 9781032836508.

https://doi.org/10.1201/9781003659983

© 2026 The Authors. Published by CRC Press. This is an author produced version of a chapter published in Railway Engineering Technology: Developments and Innovations. Uploaded in accordance with the publisher's self-archiving policy.

Reuse
Items deposited in White Rose Research Online are protected by copyright, with all rights reserved unless indicated otherwise. They may be downloaded and/or printed for private study, or other acts as permitted by national copyright laws. The publisher or other rights holders may allow further reproduction and re-use of the full text version. This is indicated by the licence information on the White Rose Research Online record for the item.

Takedown
If you consider content in White Rose Research Online to be in breach of UK law, please notify us by emailing eprints@whiterose.ac.uk including the URL of the record and the reason for the withdrawal request.





Adaptive sliding mode controller development to improve rail network efficiency through virtual coupling: a case study evidence

Saikat Dutta

https://orcid.org/0000-0002-9906-6477

Abstract

Virtual coupling is a novel approach to train operation, maintaining safe separation between trains by accounting for both braking distances and a safety factor. This control strategy aims to enhance rail network efficiency by allowing trains to couple and decouple while in motion or at stations, ultimately improving speed and flexibility. However, its implementation involves overcoming substantial challenges in controller design to prevent collisions, particularly under emergency braking. This chapter explores virtual coupling's benefits over conventional systems, presenting a MATLAB/Simulink simulation framework that models virtually coupled trains across varied scenarios. It focuses on the Calder Valley line between Leeds and Sowerby Bridge on the UK Rail Network's North & East route. This study is motivated by high daily commuter volumes in West Yorkshire's urban hubs (Leeds, Bradford, Halifax) and extends to Sowerby Bridge to assess potential added flexibility. Specifically, for trains operated by Northern Rails, an adaptive sliding model control algorithm is developed, factoring in existing communication infrastructure. By modelling and integrating communication delays into controller design, results indicate this system's promise to increase network capacity, efficiency, and safety.

Keywords: Virtual Coupling, Adaptive Sliding Mode Controller, Train Control System, Adaptive Control, Simulation Framework

Introduction

The concept of virtual coupling is attracting research interest lately as a next-generation train control operation. In this system, the train control is done entirely by cab-based signalling elements and it relies on the vehicle to vehicle communications. Various case study scenarios and roadmaps on how virtual coupling can be introduced into the network are studied (Goikoetxea 2016, Aoun, Quaglietta and Goverde 2020).

The current focus of the Railways is on enhancing capacity through the construction of high-speed routes, light rail networks, and the integration of additional trains into the network, aiming to accommodate a projected 15% rise in passenger numbers by March 2024 in the UK (Network Rail 2018). One proposed solution involves reevaluating train control systems and virtually coupling trains to increase the number of trains operating within the existing network.

This new control system promises to enhance the rail network by enabling virtual coupling and decoupling of trains during operation. Similarly, it aims to optimise road networks by facilitating train platooning in the same direction, thereby improving overall network efficiency. However, this alternative approach brings forth new challenges related to controller development and train operation systems.

State of Art: Automatic Train Control

To ensure system safety, rail networks employ various standards of Automatic Train Control systems, predominantly utilising fixed-block signalling across most operational areas worldwide. A newer development, the moving-block system, is also deployed in limited operational environments. Fixed-block signalling divides tracks into fixed-length blocks, establishing safe gaps between trains. Only one train is permitted to occupy a block at any given time. The fixed length of these blocks restricts flexibility within the network, aiming primarily to enhance reliability and safety while improving network speed.

In the European rail network, the European Train Control System (ETCS) is employed, utilising fixed-block signalling in both Level 1 and Level 2 systems. Level 2 ETCS introduces cab-based signalling, where train position is communicated via cab-based radio, while Movement Authority is generated by interlocking systems. Despite these advancements, train positioning continues to rely on trackside balises and adhere to the fixed-block system.

The limitation of not allowing a second train into a section of track defined by the fixed blocks installed, until that is free, restricts the capacity improvement of the network. In the Moving Block Signalling system [shown in Fig. 1] the track is considered as a continuous line, and it allows trains to run at a safe distance to each other rather than restricting them by the pre-defined blocks. The safe distance between two trains depends on the speed of the trains, which allows to reduce the gap in low speed. Moving block is in operation in a few urban railways including the Victoria Line, Jubilee line of London Underground, Hong Kong MTR, New York City Subway's BMT Canarsie Line.

ETCS level 3 system, which is in the development stage, operates with fully radio-based communication where the trains transmit information with Radio Block Centre (RBC) without any trackside equipment. Thus, ETCS Level 3 operates in the moving block principle by considering the track as a continuous element rather than dividing into smaller blocks. The balises are still used to report the position of the train to maintain train integrity. This shift towards a moving block principle in ETCS Level 3, combined with the continuous track monitoring, opens the door for advanced technologies like virtual coupling, which can significantly enhance track capacity, improve operational efficiency, and ensure better safety by allowing trains to operate more closely and dynamically.

<Figure 1.1 here>

Figure 1.1. Moving Block Signalling and Virtual Coupling System

The Concept: Virtual Coupling

Virtual coupling was inspired by the car-following model initially proposed for road transport, where multiple vehicles coordinate in a platoon relying on vehicle-to-vehicle (V2V) communications. Following this concept, autonomous rail vehicles can be run to operate in close proximity within a platoon. A critical aspect of such platoons, which are connected (or coupled) virtually is the need for a controller to coordinate the movements of individual vehicles or trains to prevent collisions.

The concept of coupling a set of trains while running and decoupling near the switches/ or stations as required is a potential way to increase the capacity of the network. The virtually coupled trains run as a single coupled train with multiple equally spaced smaller trains. The much smaller gap between two smaller trains ensures more trains on a length of track compared to fixed block or moving block systems [See Fig. 1].

In the moving block signalling system, the gap between trains is determined based on the distance it takes for the trains to come to a stop in an emergency. However, this gap could be reduced further if it is based on real-time information about what the train in front is doing and where it will stop if it hits the brakes. In the concept of virtual coupling, two trains communicate information about their changing speed and brake activity so that they can decrease or increase the gap accordingly between them to the minimum necessary.

From a control perspective, studies (Bauso, Fecarotti and Khaleghi 2023, Zhu, Huang et al. 2023) have introduced cooperative controls into moving block models to enhance the safety performance of multiple train operations. These studies incorporate similar controller components to virtual coupling but still rely on absolute braking distance. Thus, studying different controllers and developing an adaptive controller is one of the needs for the virtually coupled trains.

Advantages and Limitations of Virtual Coupling

Virtual coupling, as previously mentioned, is a control strategy that mimics a mechanical link between systems that are physically separated. In train control, this approach creates the effect of trains being coupled together, even though they are not physically connected. This is achieved through control algorithms that synchronize the movements of the trains, ensuring their safe and efficient coordination during operation. To better understand the difference, advantages and limitations of virtual coupling over moving block signalling has been discussed here.

The key difference between virtual coupling and moving block signalling is in their approach to train control. Moving block signalling depends on predefined track segments and strict block occupancy rules. In contrast, virtual coupling employs advanced algorithms to enable a more flexible and efficient operation, allowing trains to coordinate more dynamically.

Moving block signalling offers a concept that is relatively easy to implement while providing a designated level of safety. Virtual coupling, on the other hand, significantly enhances operational efficiency by allowing for higher train densities and shorter headways, thereby increasing capacity. Virtual coupling offers greater flexibility, making it adaptable to various operational scenarios such as dynamic speed limits or priority assignments. This system can also reduce energy consumption by optimising train movements, leading to more efficient operations.

Virtual coupling, though highly efficient, presents certain challenges. It requires complex control algorithms and advanced infrastructure, making implementation more difficult. The initial and ongoing costs of deploying virtual coupling systems are generally higher than those of traditional systems. Additionally, reliance on modern technology and communication systems introduces potential reliability concerns, as failures could disrupt operations. However, with ongoing advancements in mechatronic switches, mechatronically guided vehicles over switches, and enhanced 5G communication in railways, these challenges are expected to be overcome in the near future.

Recent Trends in Virtual Coupling

In recent years, considerable research has focused on advancing virtual coupling control systems for trains. A proof of concept for Virtual Coupling is presented within the European Rail Traffic Management System (ERTMS/ETCS) framework, along with a coupling control algorithm that accounts for time-varying communication delays, supported by numerical analysis from a case-study simulation (Mitchell, Goddard et al. 2016). Early research demonstrated this concept forms the basis for modern virtual coupling control systems. In the context of Japan's high-speed Shinkansen network, solutions have been proposed to facilitate coupling and uncoupling of trains during operation, improving the line capacity of the network (Schumann 2016). The effectiveness of this approach was verified using

DFSimu, a simulation tool developed by the German Aerospace Center (DLR) (Homay, de Sousa and Almeida 2017).

Further feasibility analyses have also identified longitudinal control as a critical element of virtual coupling. Flammini et al.(Flammini, Marrone et al. 2018) proposed decentralized control strategies based on simplified third-order models of train dynamics in state space. These strategies rely on local actions determined from on-board measurements and information from adjacent trains and infrastructure, while also considering time-varying communication delays and errors.

Model Predictive Control (MPC) has been widely used in virtual coupling simulations (Felez, Kim and Borrelli 2019, Chen, Xun and Liu 2020, Luo, Tang et al. 2021). In particular, Felez et al. (Felez, Kim and Borrelli 2019) explored the use of Model Predictive Control (MPC) to manage virtually coupled trains, achieving a significant reduction in tracking distances. However, determining the optimal tracking distance to maximize line capacity while ensuring safety remains an open challenge. Other approaches including constraint-force-driven controllers based on the Udwadia-Kalaba method (Wang, Yang et al. 2022), PID controllers (Duan, Yang et al. 2020, Rawlings, Dutta and Dixon 2022, Qiu, Li et al. 2023, Wu, Ge et al. 2023) have also been explored. All these methods have been proposed and shown to reduce communication delays, further enhancing system performance.

However, very few studies have focused on developing sliding mode controllers specifically for virtually coupled trains. Park et al. (Park, Lee and Eun 2020) introduced a gap controller based on sliding mode control for a nonlinear train model with uncertainties, alongside a gap reference generation scheme to manage train merging and separation while adhering to acceleration and jerk constraints. This study addresses position and velocity measurement errors due to wheel diameter inaccuracies by proposing an error correction scheme, both of which are validated through simulations. However, it did not address longer couplings or the impact of parameter uncertainties, which may necessitate the use of adaptive controllers. This study demonstrates the potential of using a sliding mode controller to manage the different modes of virtual coupling: coupling, running, and decoupling.

Adaptive Sliding Mode Control (ASMC) has shown significant potential in truck platooning by effectively handling uncertainties, disturbances, and varying system parameters that are common in such dynamic environments (Yadav, Sankaranarayanan and Roy 2021, Zhu, Li et al. 2022). ASMC can adaptively adjust the control law in response to changes in truck dynamics (e.g., varying loads or road conditions), ensuring robust performance and stability across the platoon. Its ability to mitigate chattering, a common issue in traditional sliding mode control, while maintaining strong disturbance rejection and trajectory tracking, makes it particularly suitable for ensuring smooth and coordinated movement in truck platoons. Kwon and Chwa (2014) (Kwon and Chwa 2014) highlights the importance of the bidirectional strategy in platoon control by demonstrating that, despite its previous drawbacks compared to the leader-predecessor strategy, it offers a more feasible implementation in actual systems, with their proposed adaptive bidirectional control method showing improved performance and guaranteed string stability. Similar work has been demonstrated by Goli et al. (Goli and Eskandarian 2014), where a platoon operates

using a bidirectional controller that incorporates information from both preceding and following vehicles.

Considering the robustness to uncertainty and disturbances, and fast response, adaptability, ASMC is chosen as a more preferred solution than MPC as train controller. An adaptive SMC is designed to be robust against uncertainties in the system dynamics and external disturbances; whereas MPC is reliant on accurate model parameters. MPC, while effective for systems with accurate models, can be less robust to uncertainties. In addition, In Adaptive Sliding Model Control systems the system's trajectories to converge to a sliding surface, ensuring rapid and stable responses. This is essential for virtual coupling applications where quick and accurate tracking of desired coupling behaviour is required. Whereas MPC's optimisation-based approach is slower in response due the process involved. Moreover, MPC requires more complex computations, involving optimisation and prediction horizons, which makes them computationally heavy. Thus, Adaptive Sliding Mode Control (SMC) offers a good combination of robustness, fast response, adaptability, and simplicity, making it a well-suited choice for virtual coupling application.

Given the challenges associated with very short following distances, high speeds, and heavy train masses, controller accuracy and robustness are critical. Simplifications in controller development mean that railway operators demand rigorous validation before real-world implementation. Thus, the need for adaptive bidirectional control arises to explore improved stability and performance in platoon systems.

This chapter focuses on the development of an adaptive controller for virtual coupling systems, with the aim of maintaining string stability and ensuring safe train spacing. By minimising both track usage and spacing errors, this controller optimises operational efficiency. One of the key features of this adaptive controller is its ability to dynamically adjust to changing conditions, such as fluctuations in train speeds and network constraints, which enhances its suitability for real-world implementation. The primary innovation of this study lies in the development of an adaptive sliding mode controller. Unlike existing robust controllers, which tend to be computationally demanding, this controller offers a more efficient solution that adapts to real-time changes in the railway environment. By dynamically adjusting to varying operational conditions such as train speed variations and network constraints, it significantly enhances the flexibility and practicality of virtual coupling in high-density rail systems.

This chapter contributes to the current research landscape by advancing the practical implementation of virtual coupling technology. By enabling safe and efficient high-density train operations, this study offers a valuable solution for optimising rail networks and adds to the ongoing research efforts in mechatronic systems and adaptive control within railway engineering.

Mathematical Modelling

Train Longitudinal Model:

<Figure 2 here>
Figure 2. Schematic model of a three-coach train

Individual Train Model:

For the selected case study, we have considered a Class 195 Northern service which comprises of three coaches (DMSL-MS- DMS). Thus, first individual train governing equations have been developed to study the dynamic behaviours of the train itself. In this model, the two coaches are considered to be joined using a physical coupling, which is modelled as a combination of stiff spring and damper, and the mathematical equation has been derived as

$$m_1 \ddot{x}_1 + K(x_1 - x_2) + C(\dot{x}_1 - \dot{x}_2) = \frac{F}{2} - F_{e1} \quad (1)$$

$$m_2 \ddot{x}_2 - K(x_1 - x_2) - C(\dot{x}_1 - \dot{x}_2) + K(x_2 - x_3) + C(\dot{x}_2 - \dot{x}_3) = \frac{F}{2} - F_{e2} \quad (2)$$

$$m_3 \ddot{x}_3 - K(x_2 - x_3) - C(\dot{x}_2 - \dot{x}_3) = \frac{F}{2} - F_{e3} \quad (3)$$

$$\dot{F} = \frac{-1}{\tau}(F - u) \quad (4)$$

where, *F* is the traction/braking force by the engine; it is considered that the force is distributed equally among the two coaches, thus using (*F/2*) in the individual equations; *u* is the controlled force of traction/braking available considering the inertial effect of the system, $F_{e,i}$ are the external forces acting on coaches (*i=1,2,3*).

The parameters are listed in Tab. 1. The following assumptions were made while constructing the equations:

- the traction/braking force is distributed equally between the two coaches.
- τ is the inertial lag due to internal dynamics of the system.
- The aerodynamic force is acting on the first coach only.

The external force includes the aerodynamic force, force due to gravity in case of slopes, and force due to curving resistance as follows:

$$F_e = F_{aero} + F_g + F_R \quad (5)$$

where,

$$F_{aero,1} = m_i(B_1 + B_2 v_1 + B_3 {v_1}^2)$$

$$F_g = -m_i \, g \; slope$$

$$F_R = -\frac{6\,m_i}{R}$$

The parameters used are explained in tab. 1.

Parameters	Description	Value
m_1, m_3	Mass of the DMSL, and DMS car	41 * 10^3 kg
m_2	Mass of the DM car	39.4*10^3 kg
L_1, L_2, L_3	Lengths of the DMS, DMSL cars	24.026 m
$\boldsymbol{\tau}$	Physical Delay	0.1 s
L_C	Coupling Length	0.85 m
B_{max}	Allowable araking	0.83 m/s2
A_{max}	Allowable acceleration	0.83 m/s2
K	Coupling Bounce stiffness	80*10^3
C	Coupling Bounce damping coefficient	100*10^3
B_1	Davis Equation coefficient	0.01176 N/kg
B_2	Davis Equation coefficient	776.16 *10^(-6) N-s/ m-kg
B_3	Davis Equation coefficient	16*10(-6) N-s^2/ m^2-kg
slope	Track grade	mm/m
R	Radius of the curved track	m

Table 1. Parameters of Class 195 coaches of Northern Trains, UK running on the case study network in Manchester Victoria – Chester/Leeds Routes. (Northern Railway 2024)

Equivalent model:

In practice, the two coaches almost run as a single unit, considering the stiff physical coupling, and in this chapter, we are not considering any decoupling of the two coaches within the train. Thus, a simpler mathematical equivalent model can be developed considering equivalent mass of the two coaches as a single mass, and the following governing equations are constructed.

$$\ddot{x}_e = u - F_{Le}/m_e \qquad (6)$$

where, m_e is the equivalent mass of the vehicle, the equivalent length of the vehicle is considered as:

$$L_e = L_1 + L_2 + L_3 + 2L_C \qquad (7)$$

To compare the performance of the equivalent vehicle against the muti-carriage vehicle model, both were tested against two different traction force conditions, keeping the gravity force, and curvature force as zero.

<Figure 3 here>
Figure 3. Performance of equivalent model when subjected to pulse traction input

Fig. 3 shows that the performance of the equivalent model mimics the multibody model well, with maximum position error of 4mm for total displacement of 1.36km, which is almost negligible. The error in the velocity performance is also negligible. However, when a random traction force (Fig. 4) is applied the performance between the two model deteriorates, with velocity error that results in position error. However, for a longer time, the velocity error converges to zero which reduces the position error to a very small percentage (below 0.01m) of the total displacement.

The main objective of reducing the model complexity is the increased flexibility of the system to design the controller which can consider the individual trains as a single mass system. From now on, in this chapter, the equivalent train model will be used for study.

<Figure 4 here>
Figure 4. Error in the performance of two models when subjected to random traction input

Controller Development

To design a longitudinal controller for railway virtual coupling, we need to consider two layers of controllers. Firstly, the upper-level controller, which ensures safe operation by determining the required distance and speed, as well as calculating the control input for individual vehicles. The second layer of control focuses on generating the determined control input within the train. In this chapter, we will primarily focus on the top-level controller, assuming that the second-level controller functions as discussed in Chapter 2, accounting only for the inertia effects of the engine. We will explore various control strategies that can be applied to ensure effective virtual coupling. The performance of these controllers will be evaluated and compared against a random control input to assess their effectiveness.

<Figure 5 here>
Figure 5. Schematic of three trains [(i-1)th, i-th and (i+1)-th] in the virtually coupled system of n-trains.

PID Controller with preceding vehicle connection only

As the first control strategy, we consider a unidirectional PID controller with a spacing control policy. In this approach, the spacing between vehicles is dynamically determined by

the velocity of each vehicle relative to its preceding vehicle, as well as the relative distance between them.

A schematic representation of this system is provided in Fig. 5. In this section, we consider a system of *n* trains running in virtual coupling. The first train follows a predefined speed profile of the network, controlled by a PID controller to maintain its speed. The *i*-th vehicle in the coupling receives information only about the *(i-1)*-th vehicle (i.e., the preceding vehicle).

The relative spacing between two vehicles is defined as:

$$r_i = x_{i-1} - x_i \tag{8}$$

The spacing error is defined as:

$$e_i = r_i - SB = x_{i-1} - x_i - SB \tag{9}$$

The safety buffer (SB) is calculated based on the braking distance of the two vehicles, as well as the length of the preceding train (L). $SB_i = L + ({v_{i-1}}^2 - {v_i}^2)/2a_{b,max}$. Since all the trains have the same length, for simplicity, we omit the suffix i and use a constant L. This assumption allows us to simplify the formulation of the system without introducing additional complexity related to varying train lengths. The safety buffer can also be termed as relative braking distance or movement authority (Pan, Peng et al. 2021).

The purpose of the unidirectional PID controller is to manage the virtually coupled vehicle series, ensuring that each spacing error (e_i) is minimized to zero. This helps maintain the individual stability of each vehicle while also ensuring string stability across the entire system, allowing the virtual coupling to function effectively and safely.

The control law for the i-th vehicle is proposed as:

$$u_i = K_{Pi}\, e_i + K_{Di}\, \dot{e}_i + K_{Ii} \int e_i \tag{10}$$

Now, substituting the control input to the equation of motion, we can write,

$$\ddot{x}_{ei} = u_i - F_{Le}/m_{ei} \tag{11}$$

$$\ddot{e}_i = \ddot{x}_{i-1} - \ddot{x}_i = a_{i-1} - (K_{Pi}\, e_i + K_{Di}\, \dot{e}_i + K_{Ii} \int e_i - F_{Le}/m_{ei}) \tag{12}$$

Rearranging differentiating it

$$\dddot{e}_i = \dot{a}_{i-1} - K_{Pi}\, \dot{e}_i + K_{Di}\, \ddot{e}_i + K_{Ii}\, e_i \tag{13}$$

Now, to ensure the designed controller is stable, we can use Laplace transform, to determine the transfer function as

$$C(s)_i = \frac{E(s)_i}{A(s)_i} = \frac{s}{s^3 + K_{Di}\, s^2 + K_{Pi}\, s + K_{Ii}} \tag{14}$$

For the system to be stable, all poles of the characteristic equation of the transfer function of *C(s)* must have negative real parts, meaning they should lie in the left half of the complex plane. Using the Routh-Hurwitz Stability Criterion, we chose the control parameters K_{Pi}, K_{Di}, and K_{Ii} such that:

$$K_{Pi}, K_{Di}, K_{Ii} > 0 \\ K_{Pi}, K_{Di} > K_{Ii} \quad (15)$$

These conditions guarantee that all the poles of the system have negative real parts, ensuring stability.

<Figure 6 here>

Figure 6. Control architecture of uni-directionally coupled trains.

To ensure the designed controller is string stable, we need to consider he amplification of error as it propagates through virtually coupled system. It is crucial for safety, performance, and scalability to design a formation control architecture that ensures disturbances propagate in a uniformly bounded manner. For any general interconnection of nonlinear systems, string stability is defined as a requirement that the states of the entire system remain bounded over time and spatial index whenever the initial conditions are bounded. The entire system is considered string stable if

$$|G_i(s)|_\infty = \frac{|E_i(s)|_\infty}{|E_{i-1}(s)|_\infty} \leq 1 \quad (16)$$

To derive the expression for $G_i(s)$, we analyse the control architecture of the given system, as illustrated in Fig. X. The system is structured as follows:

$$E_i(s) = \frac{C\,H}{1+C\,H} E_{i-1}(s) \text{ and } E_2(s) = \frac{1}{1+C\,H} E_1(s) \quad (17)$$

It can now be noted that the system to become stable, $\frac{1}{1+CH}$ needs to be small. In addition, $|G_i(s)|_\infty \leq 1$ condition needs to be satisfied. These two conditions cannot be guaranteed at all the given frequencies (Shaw 2005). Thus, uni-directional PID controller with the information from the preceding vehicle only, is unable to provide the string stability of the system.

PD Controller with preceding and following vehicle connection

Considering the same system depicted in Fig. X, a new control architecture has been developed to account for communication between both preceding and following trains. The control law for i-th train is now designed.

$$u_i = \begin{cases} K_{PFi}\, e_i + K_{DFi}\, \dot{e}_i - K_{PF(i+1)}\, e_{i+1} - K_{DF(i+1)}\, \dot{e}_{i+1} & for\ i = 1,2, \dots (n-1) \\ K_{PFn}\, e_n + K_{DFn}\, \dot{e}_n & for\ i = n \end{cases} \quad (18)$$

The last train, i.e, n-th train requires a modified control law in absence of the preceding vehicle, and only one reference train communication is used to design this.

Considering the time constant for the system dynamics, τ is can be shown that the system is stable if $(K_{DB} - \tau K_{PB}) > 0$

The string stability condition can also be achieved by satisfying the conditions (Ghasemi, Kazemi and Azadi 2013):

$$\begin{aligned} K_{PB} - \frac{D_P}{\sqrt{2}} &> 0 \\ K_{DB} - \frac{\tau}{4} + \frac{D_D}{2} &< 0 \\ (K_{DB})^2 &> 2\,K_{PB} + D_P + \frac{{D_D}^2}{2} \end{aligned} \tag{19}$$

where, $D_P = K_{PF} - K_{PB}$ and $D_D = K_{DF} - K_{DB}$.

Adaptive Sliding Mode Controller (ASMC)

As it has been established that the bidirectional control law is best suited to achieve stability, an adaptive sliding mode controller has now been designed for the virtual coupling. We consider the same virtually coupled train system depicted in Fig. 5, with n trains, where the first train follows the reference velocity of the network using a PID controller (as per the uni-directional case). We now designed the sliding surface as,

$$\sigma_i = s_i e_i + \dot{e}_i = s_i e_i + (\dot{x}_{i-1} - \dot{x}_i)$$

where $s_i > 0$ for each train and considered constant in this series of trains.

Since the information from the preceding and following vehicles can be filtered to obtain their time derivatives, it is reasonable to assume that the time derivatives of position and velocity are available without any loss of generality. Furthermore, because the convergence of the sliding surface for the i-th train doesn't ensure string stability, we need to design a composite sliding surface for the i-th vehicle with communication from preceding and following vehicles. This can be achieved as follows:

$$\sum_i = \begin{cases} \lambda_i \sigma_i - \sigma_{i+1} & i = 1,2 \ldots, n-1 \\ \lambda_n \sigma_n & i = n \end{cases}$$

Where, $\lambda_i$is a positive constant. For this problem, where the train parameters are considered similar, we have chosen λ_i as constant for all the trains, thus ignoring the index *i* from now on.

Lemma 1: $\sum_i$ becomes zero for all *i=1,2,..n; if and only if* $\sigma_i$becomes zero for all *i=1,2,..n* at the same time. This holds because $\sum_i = \lambda\sigma_i - \sigma_{i+1}$with $\lambda > 0$, and $\sum_{n+1}$doesn't exist and considered as zero to construct the combined sliding surface.

Proof: We can now generate the relationship between σ and $\sum$ as:

$$\sum = \Lambda\sigma$$

where,

$$\Lambda = \begin{bmatrix} \lambda & -1 & \dots & 0 & 0 \\ 0 & \lambda & \cdots & 0 & 0 \\ \vdots & \vdots & \ddots & \vdots & \vdots \\ 0 & 0 & \cdots & \lambda & -1 \\ 0 & 0 & \cdots & 0 & \lambda \end{bmatrix}$$

$$\sum = [\sum_1 \quad \sum_1 \quad \dots \quad \sum_n]^T$$

$$\sigma = [\sigma_1 \quad \sigma_1 \quad \dots \quad \sigma_n]^T$$

Now, it can be noted that λ is positive constant, which makes the matrix Λ an invertible matrix. Thus, $\sum$ becomes zero for all σ_i become zero.

According to Lemma, the control law is designed to guarantee that the Composite Sliding Surface (CSS) converges to zero. The time derivative of $\sum_{\mathrm{i}}$ becomes:

$$\dot{\sum}_i = \lambda\dot{\sigma}_i - \dot{\sigma}_{i+1} = \lambda\,[s_i\dot{e}_i + (\ddot{x}_{i-1} - \ddot{x}_i)] - [s_i\dot{e}_{i+1} + (\ddot{x}_i - \ddot{x}_{i+1})]$$

This can be rewritten as

$$\dot{\sum}_i = -\frac{\lambda+1}{m_e}\,(u_i - F_{Lei}) + \Theta_i$$

where,

$$\Theta_i = \lambda\ddot{x}_{i-1} + \ddot{x}_{i+1} + s_i\,[\dot{e}_i - \dot{e}_{i+1}]$$

Now, based on this, we design the bidirectional adaptive control law for i-th train as

$$\mathrm{u}_i = \begin{cases} \hat{F}_i + \frac{\hat{m}_{ei}}{\lambda+1}\Theta_i + \frac{\mu}{\lambda+1}\sum_{\mathrm{i}} + \frac{\bar{\mu}}{\lambda+1}sgn(\sum_{\mathrm{i}}) & for\ i = 1,2,\dots.(n-1) \\ \hat{F}_n + \frac{\hat{m}_{en}}{\lambda}\Theta_n + \frac{1}{\lambda}\,[\mu\sum_{\mathrm{n}} + \bar{\mu}\,sgn(\sum_{\mathrm{n}})] & for\ i = n \end{cases}$$

here, $\hat{F}_i$and $\hat{m}_{ei}$are estimates of $F_{Le}$and m_e; the constants μ and $\bar{\mu}$ are selected to ensure the stability.

The adaptation laws for $\hat{F}_i$ and $\hat{m}_{ei}$ are obtained as

$$\hat{F}_i = \begin{cases} \zeta_F(\lambda+1)\sum_{\mathrm{i}} & for\ i = 1,2,\dots.(n-1) \\ \zeta_F\,\lambda\sum_{\mathrm{n}} & for\ i = n \end{cases}$$

$$\hat{m}_{ei} = \zeta_m\,\Theta_i\sum_{\mathrm{i}} \qquad for\ i = 1,2,\dots..n$$

The two constants, $\zeta_m$and ζ_F are positive constants that regulate the rate of adaptation.

The adaptive mechanisms adjust the parameters $\hat{F}_i$and $\hat{m}_{ei}$in real time based on the current state of the system. These estimates are continuously updated to account for variations in

the system dynamics and external disturbances. By doing so, the controller maintains high performance and stability under varying operational conditions. The positive constants, ζ_m and ζ_F determine the responsiveness of the adaptation, ensuring that the estimates converge to their true values, thereby improving the overall system's robustness and adaptability.

The convergence of the combined sliding surface can be guaranteed by satisfying the convergence requirements, which are shown in Appendix 1.

Comparison of Controller Performance

To compare the performance of the controllers, a random velocity profile has been generated and applied to train 1.

The results, shown in Figure 7, illustrate the performance of five trains following the random velocity profile when using a unidirectional PID controller. It can be observed that the trains are able to follow the preceding trains under normal conditions. However, in the presence of disturbances, such as changes in the velocity profile, the overall stability of the system deteriorates. Consequently, the velocity tracking is not as expected, and the relative distance between the trains continues to increase due to unstable behaviour.

<Figure 7 here>

Figure 7. Control performance of Virtual coupling with PID controller with preceding train information only.

Fig. 8 shows the performance of the virtually coupled system using a bidirectional PD controller. The velocity plot in Fig. 8 indicates that trains 2 through 5 run together with reduced relative distances between them. Since the control force is calculated using information from two neighbouring trains, the initial acceleration of train 2 from a stationary state is slower than expected, leading to an initial spacing error. The spacing error is lower compared to that in Figure 6. The zoomed-in view of the braking distance shows that the spacing error consistently exceeds the braking distance, ensuring the system remains safe. However, the system remains stable, as evidenced by the fact that the relative distances do not increase over time, even in the presence of a changing velocity profile, as shown in Figure 8.

<Figure 8 here>

Figure 8. Control performance of Virtual coupling with bi-directional PD controller with preceding and following train information.

For the designed adaptive sliding mode controlled virtually coupled train systems, performance demonstrates a clear improvement (Fig. 9). The velocity plot reveals that trains

2 through 5 effectively track the velocity profile, and the coupling remains stable even with changing speed profiles. Additionally, the spacing error is significantly lower compared to that observed with other controllers.

<Figure 9 here>
Figure 9. Control performance of Virtual coupling with an adaptive sliding mode controller with preceding and following train information.

Tab. 2 illustrates the performance comparison of the three virtually coupled system. For the given reference velocity of the track. For repeatability another new set of tracks is used with different velocity profile, slope and curvatures. The performances are listed as Case 2. The performance indices are calculated as:

- Overall RMS spacing error

$$Er_{RMS} = \sqrt{\frac{\mathbf{1}}{\mathbf{4}}\sum_{t}\sum_{i=2}^{5}\boldsymbol{e_i(t)^2}}$$

- Overall RMS velocity error:

$$V_Er_{RMS} = \sqrt{\frac{\mathbf{1}}{\mathbf{4}}\sum_{t}\sum_{i=2}^{5}(v_{i-1}(t) - v_i(t))^2}$$

- Total Space occupied:

$$TS_O = \sum_{t}(x_1(t) - x_5(t))$$

Index	**Case 1**			**Case 2**		
	Uni-PID	Bi-PD	ASMC	Uni-PID	Bi-PD	ASMC
$\boldsymbol{Er_{RMS}}$ (m)	442.1	392.1	152.7	535.3	402.5	161.3
TS_O (km)	10360.7	90945.4	35754.0	15360.5	84530.6	41600.1
Travel distance of train 1 (x_1) (km)	11.41	11.72	11.52	13.5	13.81	13.75
Travel distance of train 5 (x_5) (km)	9.23	9.73	10.79	11.12	11.62	12.01
$\boldsymbol{V_Er_{RMS}}$ (m/s)	2.86	6.28	1.59	5.90	4.99	1.42

Table 2. Performance comparison of the three controllers.

In Fig. 10, it is evident that the adaptive sliding mode controller optimises track usage by allowing trains to run closely together while maintaining string stability throughout the entire virtual coupling system. This approach enhances efficiency and stability, demonstrating effective management of the train series in the virtual coupling scenario.

<Figure 10 here>
Figure 10. The use of track for the three virtually coupled systems.

Framework for Coupling and Decoupling:

The virtual coupling model is developed with careful consideration of three critical phases: coupling, coupled run, and decoupling. Ensuring system stability throughout these phases is prime requirement for safe and efficient operation.

In this model, the trains, including the preceding train (i-1) and the following train (i), operate under the Moving Block signalling system. It is assumed that the states of the trains, such as position and velocity, are known to the operator, along with other essential parameters like emergency braking capabilities and allowable acceleration/deceleration. Below, we define the key terminologies used in the system checks.

- Safety Buffer for i-th train, SB_i
- End of Authority for i-th train, EoA_i
- End of Authority for coupled run, EoA_C
- Absolute Braking Distance, $AB_i = \frac{{v_i}^2}{2\,a_{max}}$
- Relative Braking Distance, $RB_i = AB_i - AB_{i-1}$

Before activating the virtual coupling mode, it is essential that the movement authority verifies that the trains involved are traveling on the same route, ensuring the feasibility and safety of the coupling process.

Coupling State

During the "Coupling" state, the first check ensures that train *i*'s position at the end of the coupling does not exceed the position of the preceding train *(i-1)*. The time required to achieve coupling depends on the velocity difference between the two trains. The time taken for train *i* to match the speed of train *(i-1)* is denoted as t_c. The condition for this check (Check 1 in Fig. 11) can be expressed as follows:

$$x_i(t_c) - SB_i < x_{i-1}(t_c)$$

where:

- $x_i(t_c)$ is the position of train i at time t_c,
- $x_{i-1}(t_c)$ is the position of train $(i-1)$ at time t_c.

This equation ensures that train *i* does not overshoot the preceding train *(i−1)* during the coupling process, thereby maintaining safe spacing. Once this check is satisfied the train *i* enters into the coupling state to reach specified speed.

Coupled Run

Train *i* must now check two critical conditions: speed and position. First, the velocity difference between train *i* and train *(i−1)* must fall within the threshold for relative velocity to allow train *i* to safely move into virtual coupling. Additionally, the spacing error of train *i* must be greater than the absolute braking distance of train *(i−1)*. This condition ensures that if train *(i−1)* initiates emergency braking at this moment, train *i* will not reach train *(i−1)*, thereby maintaining a safe separation that meets the safety threshold.

The two checks for virtual coupling are represented by the following equations:

Check 2.1 – Relative Velocity Check: The velocity difference should be within the allowable threshold for virtual coupling:

$$\boldsymbol{v_{i-1} - v_i < v_{th}}$$

Check 2.2 – Spacing Error Check: The spacing error between train *i* and train *(i−1)* must be greater than the absolute braking distance of train *(i−1)*:

$$\boldsymbol{e_i < AB_{i-1}}$$

These checks ensure both safe relative speed and sufficient distance to prevent collisions during emergency situations. Once these two checks are satisfied, the two trains start running as coupled using the adaptive sliding mode controller designed before.

Decoupling

As train *i* enters a zone near a junction, the decoupling state will be triggered. The train *I* initiates the decoupling process, and both trains revert to their original Moving Block signalling mode. When the distance to the junction falls below the spacing error, train *i* will decouple and exit the virtual coupling mode. The check equation for this decoupling condition is as follows:

Check 3:

$$\boldsymbol{d_{ji} < e_i}$$

Where, d_{ji} is the distance of the junction zone from train *i*. This condition ensures that decoupling occurs safely before the trains reach the junction, preventing any risk of collision or interference at the junction.

Similarly, while in coupling mode, train *i* continuously checks this condition (Check 4 in Fig. 11) to ensure a safe return to Moving Block signalling as it approaches a junction,

particularly in cases where virtual coupling has not been successfully achieved. This ongoing check ensures that the system transitions smoothly and safely out of virtual coupling near critical points like junctions.

To test the developed framework two test cases were developed, and the performance is tested.

<Figure 11 here>

Figure 11. Flowchart of the virtual coupling: including coupling, coupled run and decoupling phases.

Test Case 1: Variable Speed

To test this framework, the first test case is designed as a variable speed line with two stations. The simulation was conducted on a track with two stations spanning 15 km as shown by v_{ref} in the top figure at Fig. 12. The two stations are denoted by two starts at distances 3500m and 7500m. The speed limit near the station zones (shown by shaded areas) is 10m/s. The test scenario was designed to include a 60-second waiting time for the trains at the platform.

<Figure 12 here>

Figure 12. The performance of the virtually coupled trains: top – velocity of each trains along the track, middle – spacing error between the trains, bottom: position of the trains along the simulated track.

The results of the virtual coupling performance are illustrated in Figs. 12 and 13. The velocity of each train is shown to adhere to the speed limits of the simulated track, with trains successfully forming virtual couplings during the run. In the top figure of Fig. 12, it is evident that within the junction zones (indicated by the two shaded areas), the trains decouple from the virtual coupling and revert to Moving Block signalling to stop at the stations.

It is observed that the spacing error is greatest for the second train, as the first train does not use information from the second train to adjust its speed. Specifically, the Root Mean Square (RMS) spacing error between the first and second trains over the two stations is 414.3 m, while the RMS spacing error between the fourth and fifth trains is notably lower at 222.1 m. The RMS speeds of the five trains are as follows: 25.07 m/s, 25.00 m/s, 25.06 m/s, 25.06 m/s, and 25.07 m/s, respectively. These speeds indicate that coupling is well-maintained in this region, demonstrating effective coordination among the trains. Nonetheless, in all cases, the spacing error remains within safe limits, ensuring the secure operation of the system.

Test Case 2: Emergency Braking

To evaluate stability and string stability, this test case simulates a route with a speed limit of 50 mph (22.352 m/s). Train 1 performs an emergency stop at 60 seconds while in coupled mode, resuming its journey at 120 seconds and adhering to the speed limit. Another scenario occurs at 200 seconds, when Train 3 stops with an emergency brake, restarting after 90 seconds.

The results in Fig. 13 indicate the system remains stable. When Train 1 stops, following trains decelerate gradually and hold a low, constant speed to maintain safe distances. After Train 3 stops, Trains 4 and 5 decelerate as needed without impacting Trains 1 and 2.

<Figure 13 here>
Figure 13. The performance of the virtually coupled trains for test case 2.

However, since this is a simulated track, it is essential to validate these results with a real-world track. This validation will be addressed in the next section.

Case Study

The case study focuses on the Calder Valley line, which runs between Leeds and Sowerby Bridge within the UK Rail Network's North & East route. The primary objectives of this case study are to evaluate the feasibility of implementing virtual coupling on the Calder Valley line, assess its impact on network flexibility, and optimize train scheduling to enhance overall operational efficiency. Key characteristics include varied track gradients and multiple junctions, which impact train operations and signalling.

This selection is driven by the high volume of daily commuters traveling through three major urban hubs—Leeds, Bradford, and Halifax—in West Yorkshire. The Calder Valley line spans approximately 30 kms, featuring a mix of urban and rural settings. The study extends to Sowerby Bridge to explore the potential for adding flexibility to the network.

The Calder Valley line accommodates three different train services:

1. **Type 1 – Leeds to Sowerby**: Stops at each station along the route.
2. **Type 2 – Leeds to Sowerby**: Skips stations Bramley (Station 1) and Low Moor (Station 4).
3. **Type 3 –Leeds to Halifax**: Stops at all station till Halifax, then continues on divergent route.

For this study, five trains have been considered as:

- **First Train**: Type 2
- **Second Train**: Type 1
- **Third Train**: Type 1

- **Fourth Train**: Type 1
- **Fifth Train**: Type 3

The speed profile along the route is shown in Fig. 14, which provides an overview of the operational speeds for the trains on this line. The route details have been collated from train running timings on this line. Data for five trains of each type were collected, including speed limits and location data at various signal points along the route. This comprehensive data set provides insights into train speeds, spacing, and adherence to signalling requirements.

It is assumed that trains can switch to adjacent lines near junctions. The current switching time within the UK Rail network is approximately 7 seconds. Recent research suggests that this time is expected to decrease in the near future. This assumption is based on ongoing advancements in technology and infrastructure that aim to improve switching efficiency (Dutta, Harrison et al. 2020, Olaby, Dutta et al. 2021). In the designed case study, the minimum distance between two trains in the virtual coupling mode is always greater than (with minimum of 17 seconds) the switching time. This ensures that there is sufficient time for a train to switch lines safely without interfering with the operation of other trains.

<Figure 14 here>

Figure 14. The performance of the virtually coupled trains: a case study of Leeds-Halifax line, UK.

The performance of the virtual coupling framework on the Calder Valley line (in Fig. 14), shows the behaviour of the trains as they operate under virtual coupling control. The trains follow the virtual coupling pattern on sections of the track outside the station zones. These junction/station zones are highlighted by shaded regions in the Fig. 14, showing that the coupling is maintained during regular operation but decouples near stations to allow for independent stopping and starting.

The trains are restricted by the velocity profile of the track, ensuring that they adhere to the speed limits imposed by the network. This helps maintain safety and smooth operation across the network. Even after train 1 skips a stop at Bramley (Station 1), the entire system regains its coupled formation. However, there is a noticeable increase in the gap between the first two trains. This is attributed to the low-speed limits on the network, which restricted the motion of train 2 and prevented it from closing the gap immediately after the skipped stop.

Despite the high potential capacity of the network, the current configuration demonstrates low usage of track. The system's performance highlights that while virtual coupling can enhance train coordination, the low-speed limits and operational constraints of the network prevent it from reaching its full capacity potential.

These observations provide valuable insights into the practical application of virtual coupling in a real-world scenario, pointing to areas where improvements in infrastructure or speed limits could further enhance the network's performance.

Conclusions

Virtual coupling offers a step-change approach to train operations by allowing closely spaced trains to travel together in a coordinated manner, effectively increasing network capacity without the need for significant infrastructure expansion. This is particularly important in high-density rail corridors where conventional fixed or moving block signalling systems limit train frequency and reduce operational flexibility. By enabling dynamic adjustment of train spacing, virtual coupling enhances efficiency, reduces delays, and improves overall network performance, making it a key innovation for the future of rail transportation.

It is shown through this chapter, that the adaptive sliding mode controller is able to maintain string stability within the virtual coupling system. It ensures that trains remain safely spaced while minimising track usage and spacing errors. This controller adapts to changing conditions, such as variations in train speeds and network constraints, to maintain the coupling safety. As demonstrated in the simulations, the adaptive sliding mode controller effectively manages the trade-off between operational efficiency and safety, enabling high-density train operations with minimal disruption.

The case study on the Calder Valley line demonstrates the practical application of virtual coupling in a real-world scenario. While the virtual coupling framework shows promise in improving train coordination and capacity, the study highlights several challenges, including the impact of low-speed limits and infrastructure constraints on network performance. Despite these limitations, the system has demonstrated effective coupled formation and spacing management, particularly outside station/junction zones. To unlock the full potential of virtual coupling, further improvements in network infrastructure and operational policies are necessary.

Future Research Direction:

This case study establishes a foundation for future research and implementation aimed at optimising rail network performance through advanced control strategies like virtual coupling. As the aim of this chapter is control strategy development, validation is currently confined to simulation environments only. To enhance this, the author is developing a scaled experimental setup to collect representative datasets for validation.

Future research could explore the integration of the proposed control system with emerging technologies, such as self-guided mechatronic bogies, self-adjusting switches, and advanced communication networks. Additionally, the current model does not rigorously account for time delays in state measurement and estimation, incorporating a unit delay in sensor data. A more analytical method should be developed to address these practical considerations in

future studies. Overall, these directions aim to ensure that the proposed control systems are safe, practical, and aligned with future advancements in railway technology.

Reference list

Aoun, J., E. Quaglietta and R. M. Goverde (2020). "Investigating market potentials and operational scenarios of virtual coupling railway signaling." Transportation research record **2674**(8): 799-812.

Bauso, D., C. Fecarotti and A. Khaleghi (2023). "Cooperative control and stability analysis for virtual coupling of rail vehicles." Control Engineering Practice **133**: 105452.

Chen, M., J. Xun and Y. Liu (2020). A coordinated collision mitigation approach for virtual coupling trains by using model predictive control. 2020 IEEE 23rd International Conference on Intelligent Transportation Systems (ITSC), IEEE.

Duan, H., Y. Yang, Y. Duan and J. Zhang (2020). Research on virtual coupling train operations based on moving-block and vehicle-to-vehicle communication. Journal of Physics: Conference Series, IOP Publishing.

Dutta, S., T. Harrison, C. P. Ward, R. Dixon and T. Scott (2020). "A new approach to railway track switch actuation: Dynamic simulation and control of a self-adjusting switch." Proceedings of the Institution of Mechanical Engineers, Part F: Journal of Rail and Rapid Transit **234**(7): 779-790.

Felez, J., Y. Kim and F. Borrelli (2019). "A model predictive control approach for virtual coupling in railways." IEEE Transactions on Intelligent Transportation Systems **20**(7): 2728-2739.

Flammini, F., S. Marrone, R. Nardone, A. Petrillo, S. Santini and V. Vittorini (2018). Towards railway virtual coupling. 2018 IEEE International Conference on Electrical Systems for Aircraft, Railway, Ship Propulsion and Road Vehicles & International Transportation Electrification Conference (ESARS-ITEC), IEEE.

Ghasemi, A., R. Kazemi and S. Azadi (2013). "Stable decentralized control of a platoon of vehicles with heterogeneous information feedback." IEEE Transactions on Vehicular Technology **62**(9): 4299-4308.

Goikoetxea, J. (2016). Roadmap towards the wireless virtual coupling of trains. Communication Technologies for Vehicles: 10th International Workshop, Nets4Cars/Nets4Trains/Nets4Aircraft 2016, San Sebastián, Spain, June 6-7, 2016, Proceedings 10, Springer.

Goli, M. and A. Eskandarian (2014). A systematic multi-vehicle platooning and platoon merging: Strategy, control, and trajectory generation. Dynamic Systems and Control Conference, American Society of Mechanical Engineers.

Homay, A., M. de Sousa and L. Almeida (2017). Nash equilibrium for proactive anti-jamming in IEEE 802.15. 4e (Emerging wireless sensor actuator technologies for I4. 0). 2017 IEEE 15th International Conference on Industrial Informatics (INDIN), IEEE.

Kwon, J.-W. and D. Chwa (2014). "Adaptive bidirectional platoon control using a coupled sliding mode control method." IEEE Transactions on Intelligent Transportation Systems **15**(5): 2040-2048.

Luo, X., T. Tang, H. Liu, L. Zhang and K. Li (2021). An adaptive model predictive control system for virtual coupling in metros. Actuators, MDPI.

Mitchell, I., E. Goddard, F. Montes, P. Stanley, R. Muttram, W. Coenraad, J. Poré, S. Andrews and L. Lochman (2016). "ERTMS level 4, train convoys or virtual coupling." IRSE News **219**: 14-15.

Network Rail (2018). CP6-Strategic-Business-Plan-Comprehensive-Executive-Summary. London.

Northern Railway. (2024). "Our train types." Retrieved 02/07/2024, 2024, from https://www.northernrailway.co.uk/before-you-travel/our-train-types.

Olaby, O., S. Dutta, T. Harrison, C. P. Ward and R. Dixon (2021). "Realisation of a novel functionally redundant actuation system for a railway track-switch." Applied Sciences **11**(2): 702.

Pan, J., Q. Peng, S. Zhan and J. Bai (2021). "Multiscenario-Based Train Headway Analysis under Virtual Coupling System." Journal of Advanced Transportation **2021**(1): 5642709.

Park, J., B.-H. Lee and Y. Eun (2020). "Virtual coupling of railway vehicles: Gap reference for merge and separation, robust control, and position measurement." IEEE Transactions on Intelligent Transportation Systems **23**(2): 1085-1096.
Qiu, S., N. Li, X. Wei and G. Li (2023). "Research on the stability of virtual coupling train formation based on PID controller under the influence of time delay." Transportation Safety and Environment: tdad037.
Rawlings, C., S. Dutta and R. Dixon (2022). Exploring the Virtual Coupling of Railway Vehicles. World congress of railway Research: Reshaping our railways post-pandemic: Research with an impact.
Schumann, T. (2016). "Increase of capacity on the shinkansen high-speed line using virtual coupling."
Shaw, E. E.-w. (2005). Heterogeneous string stability for vehicle formation control, University of California, Berkeley.
Wang, B., D. Yang, X. Zhang and X. Jia (2022). "Constraint-force driven control design for rail vehicle virtual coupling." Journal of Vibration and Control **28**(5-6): 551-563.
Wu, Q., X. Ge, Q.-L. Han, B. Wang, H. Wu, C. Cole and M. Spiryagin (2023). "Dynamics and control simulation of railway virtual coupling." Vehicle System Dynamics **61**(9): 2292-2316.
Yadav, R. D., V. N. Sankaranarayanan and S. Roy (2021). Adaptive sliding mode control for autonomous vehicle platoon under unknown friction forces. 2021 20th International Conference on Advanced Robotics (ICAR), IEEE.
Zhu, L., D. Huang, X. Li and Q. Wang (2023). "Cooperative operation control of virtual coupling high-speed trains with input saturation and full-state constraints." IEEE Transactions on Automation Science and Engineering.
Zhu, Y., Y. Li, H. Zhu, W. Hua, G. Huang, S. Yu, S. E. Li and X. Gao (2022). "Joint sliding-mode controller and observer for vehicle platoon subject to disturbance and acceleration failure of neighboring vehicles." IEEE Transactions on Intelligent Vehicles **8**(3): 2345-2357.

Appendix 1

Theorem:

When the adaptive control law is applied to the interconnected vehicular system, stability is achieved across the system. This stability is characterised by the following:

Sliding Surfaces (σ_i and $\sum_i$ drives toward zero, and distance error variables (e_i), which represent the deviation from the desired spacing between vehicles, are also driven to zero asymptotically.

Proof:

We first consider a Lyapunov function as:

$$V = \sum_i V_i$$

The parameter V_i is chosen as:

$$V_i = \frac{m_{ei}}{2}\sum_i{}^2 + \frac{\tilde{f}_i{}^2}{2\zeta_F} + \frac{\tilde{m}_{ei}{}^2}{2\zeta_m}$$

Where, $\tilde{f}_i$, $\tilde{m}_{ei}$ are the estimation errrors for *i*-th train.

Substituting these in the Lyapunov function and differentiating, we get,

$$\dot{V}_i = m_{ei}\sum_i \left[\frac{\lambda+1}{m_{ei}}\tilde{f}_i + \Theta_i - \frac{\tilde{m}_{ei}}{m_{ei}}\Theta_i - \frac{\mu}{m_{ei}}\sum_{\mathrm{i}} - \frac{\bar{\mu}}{m_{ei}}sgn(\sum_{\mathrm{i}}) \right] + \frac{\tilde{f}_i\,\dot{\tilde{f}}_i}{\zeta_F} + \frac{\tilde{m}_{ei}\,\dot{\tilde{m}}_{ei}}{\zeta_m}$$

$$\leq (\lambda+1)\tilde{f}_i\sum_{\mathrm{i}} + \tilde{m}_{ei}\Theta_i\sum_{\mathrm{i}} - \mu\sum_{\mathrm{i}}{}^2 - \bar{\mu}\,|\sum_{\mathrm{i}}| + \frac{\tilde{f}_i\,\dot{\tilde{f}}_i}{\zeta_F} + \frac{\tilde{m}_{ei}\,\dot{\tilde{m}}_{ei}}{\zeta_m}$$

$$= -\mu\sum_{\mathrm{i}}{}^2 - \bar{\mu}\,|\sum_{\mathrm{i}}|$$

So, overall Lyapunov function,

$$\dot{V} = \sum_i \dot{V}_i = \sum_i \{-\mu\sum_{\mathrm{i}}{}^2 - \bar{\mu}\,|\sum_{\mathrm{i}}|\,\}$$

As the value of μ is positive, the $V(t)$ is bounded for all times. Since $V_i(0)$ is bounded, and $V_i(t)$ bounded, $\sum_i$ will converges to zero.

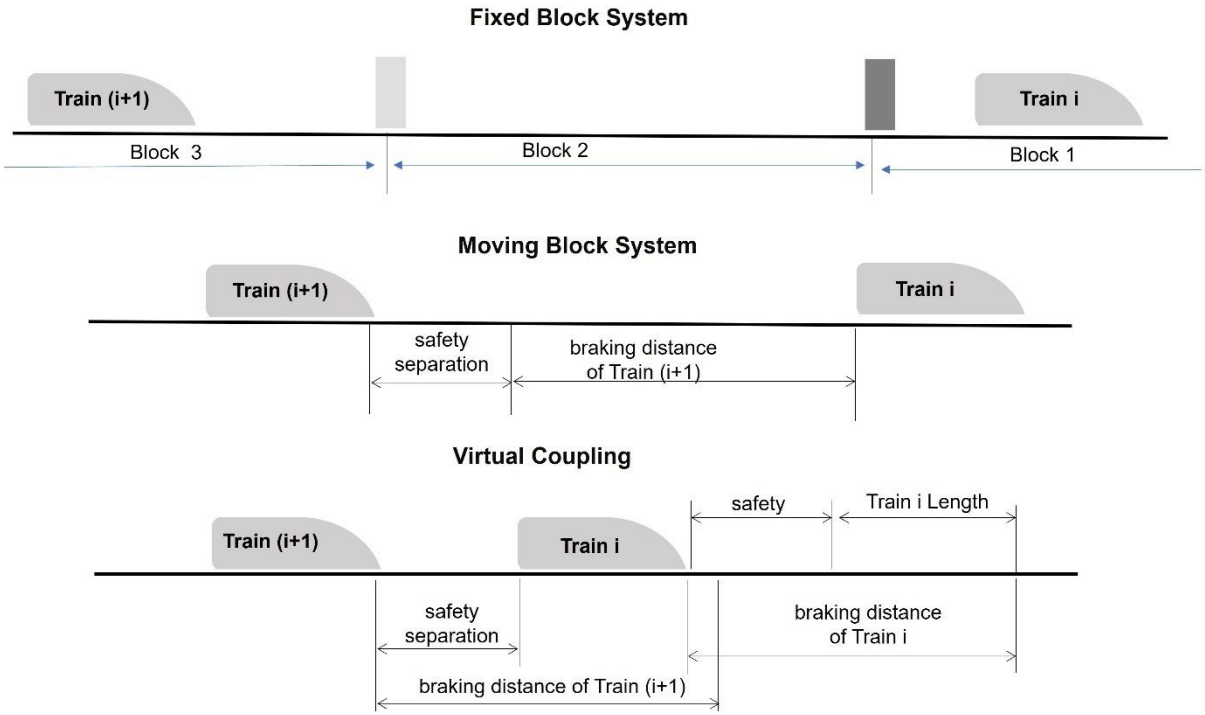


Figure 1. Moving Block Signalling and Virtual Coupling System

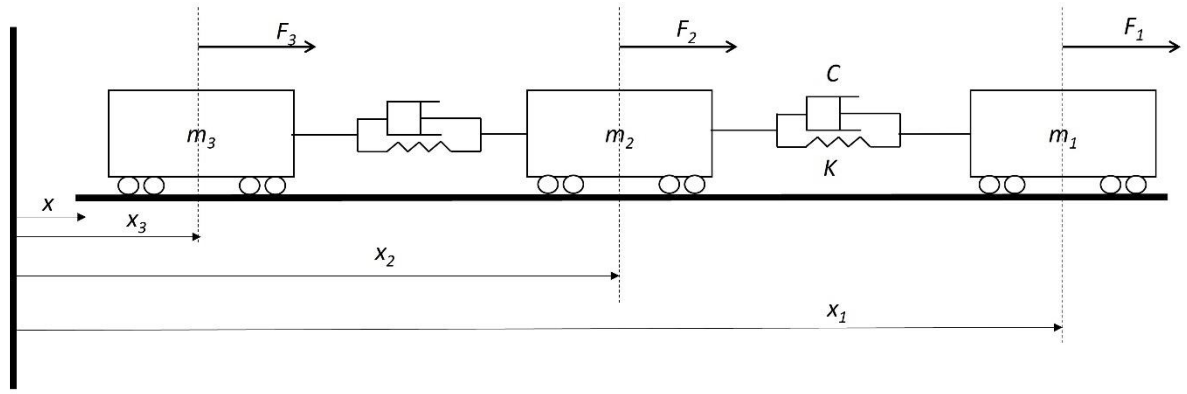


Figure 2. Schematic model of a three-coach train

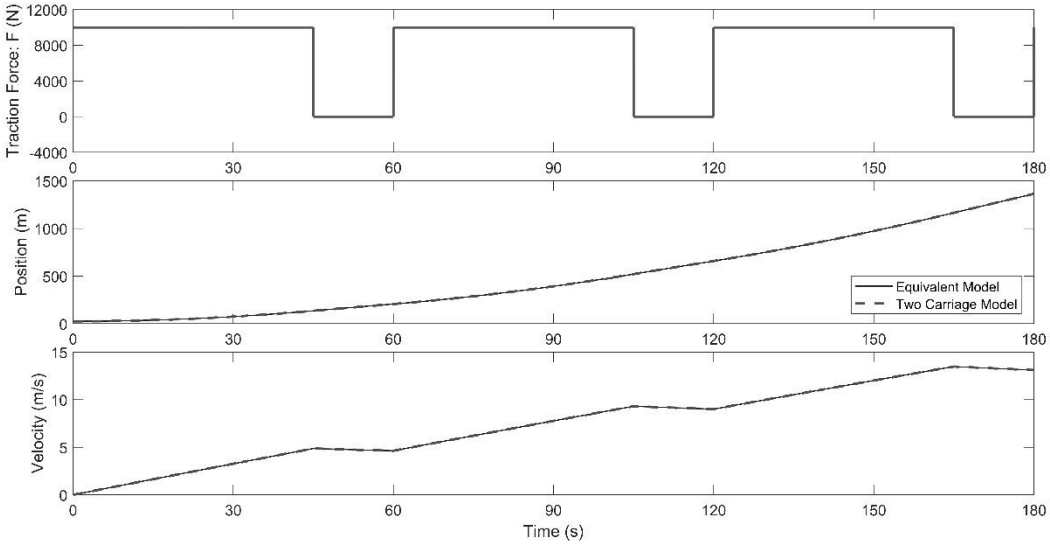


Figure 3. Performance of equivalent model when subjected to pulse traction input

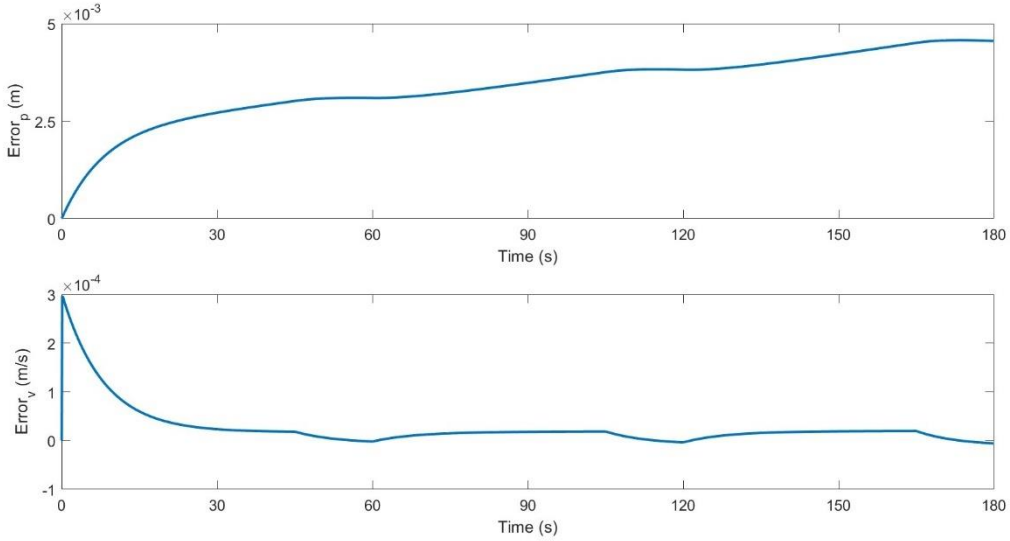


Figure 4. Error in the performance of two models when subjected to random traction input

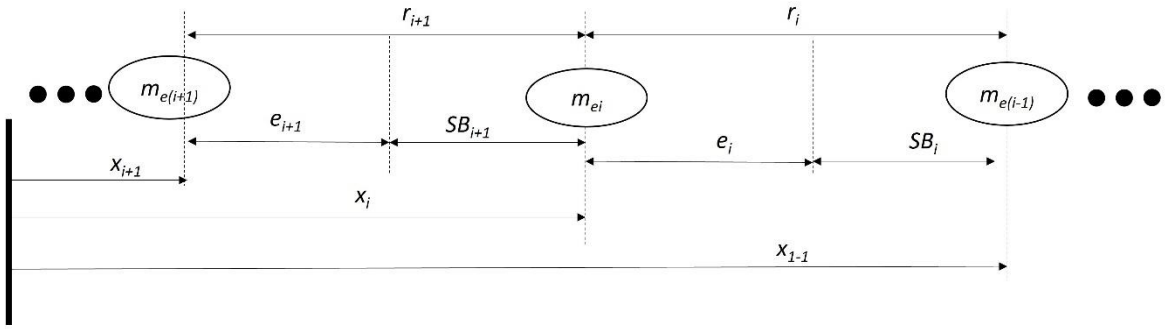


Figure 5. Schematic of three trains [(i-1)th, i-th and (i+1)-th] in the virtually coupled system of n-trains.

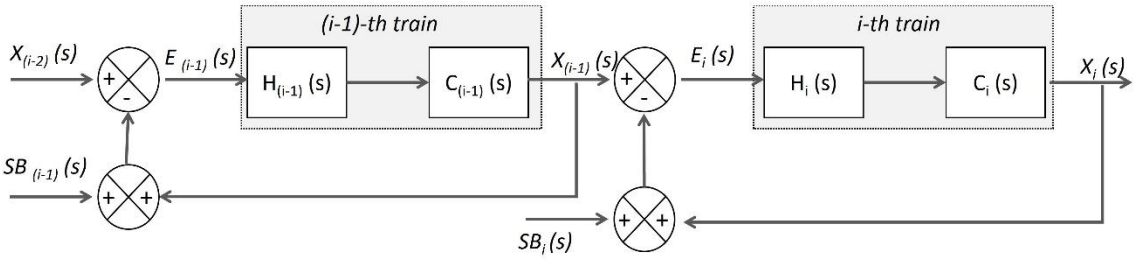


Figure 6. Control architecture of uni-directionally coupled trains.

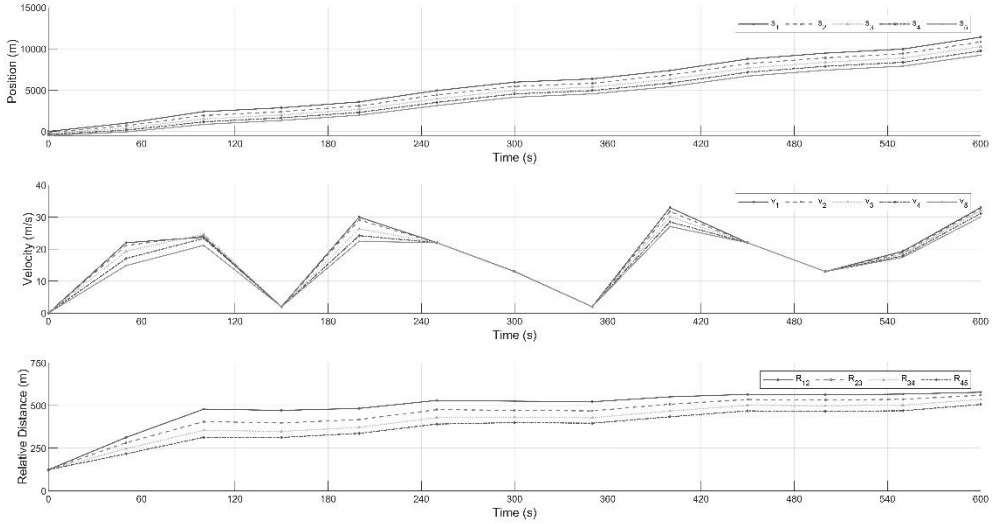


Figure 7. Control performance of Virtual coupling with PID controller with preceding train information only.

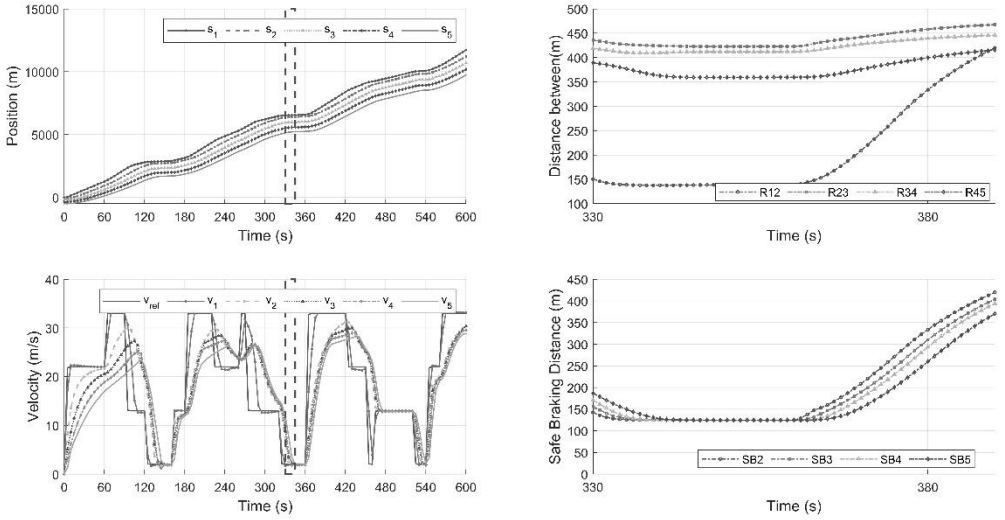


Figure 8. Control performance of Virtual coupling with bi-directional PD controller with preceding and following train information.

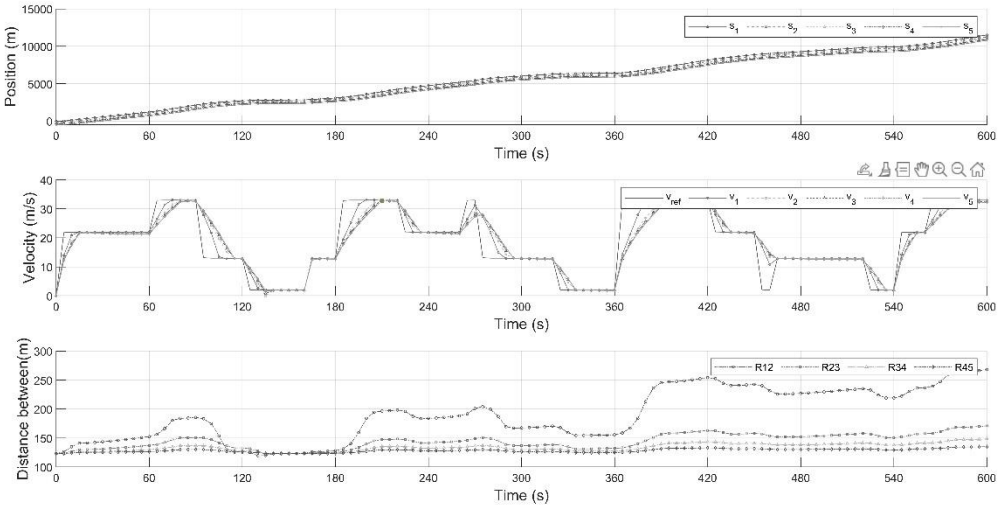


Figure 9. Control performance of Virtual coupling with an adaptive sliding mode controller with preceding and following train information.

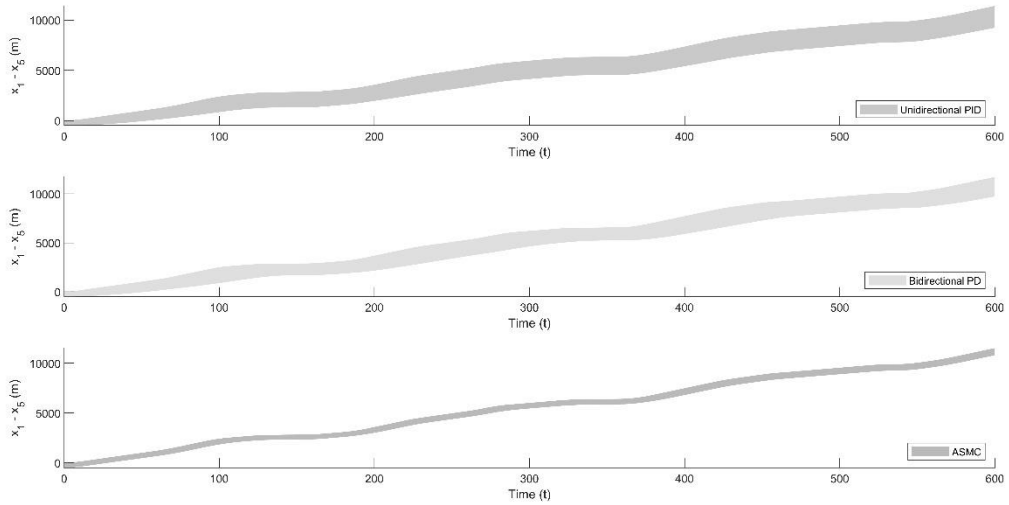


Figure 10. The use of track for the three virtually coupled systems.

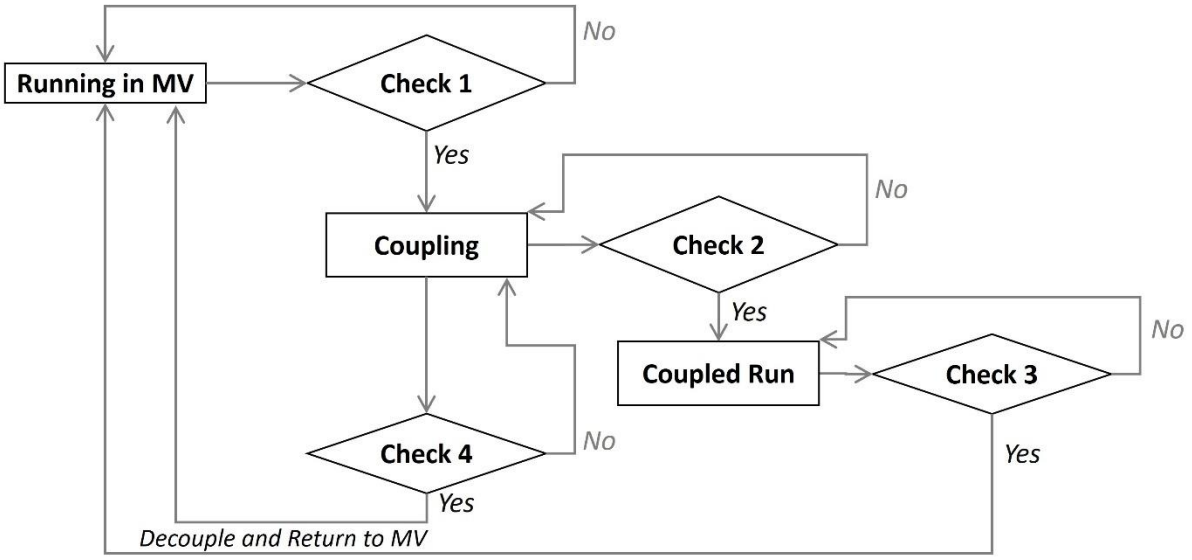


Figure 11. Flowchart of the virtual coupling: including coupling, coupled run and decoupling phases.

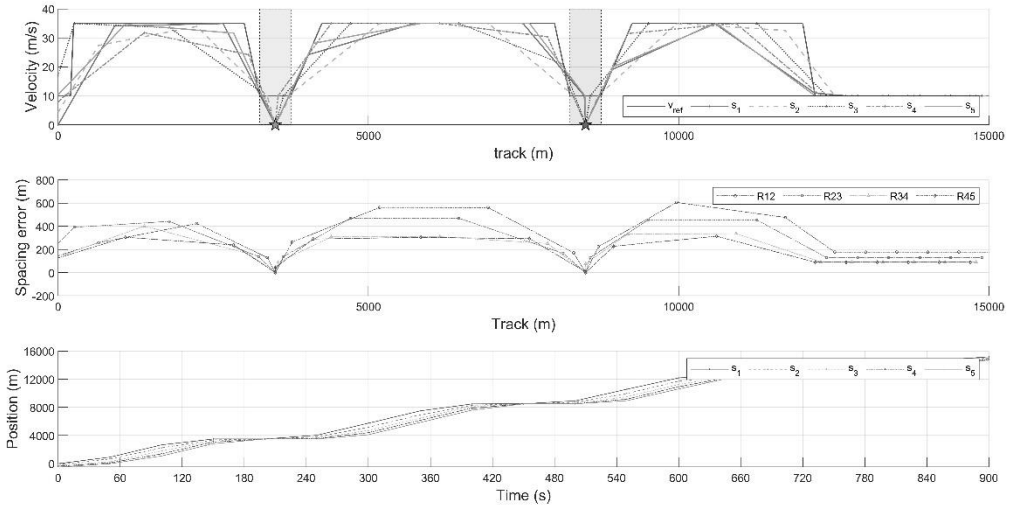


Figure 12. The performance of the virtually coupled trains: top – velocity of each trains along the track, middle – spacing error between the trains, bottom: position of the trains along the simulated track.

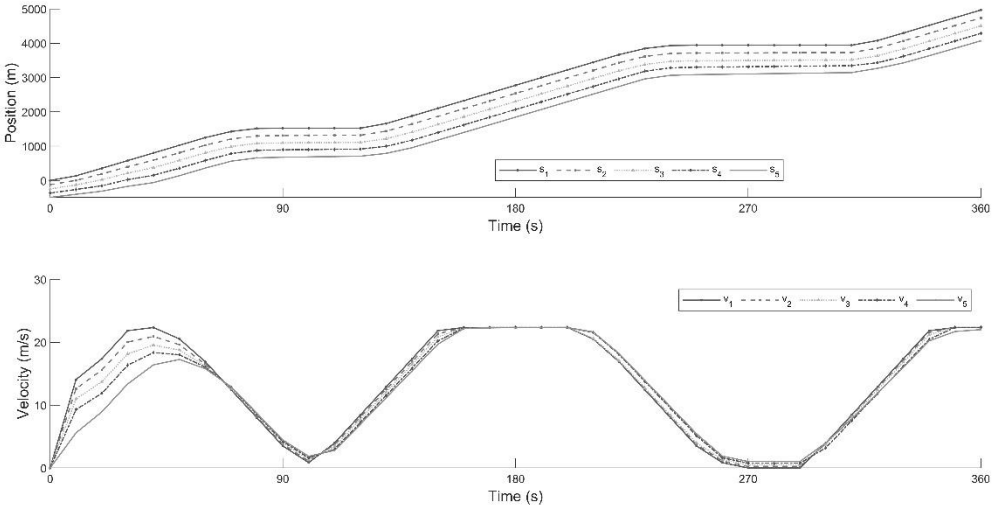


Figure 13. The performance of the virtually coupled trains for test case 2.

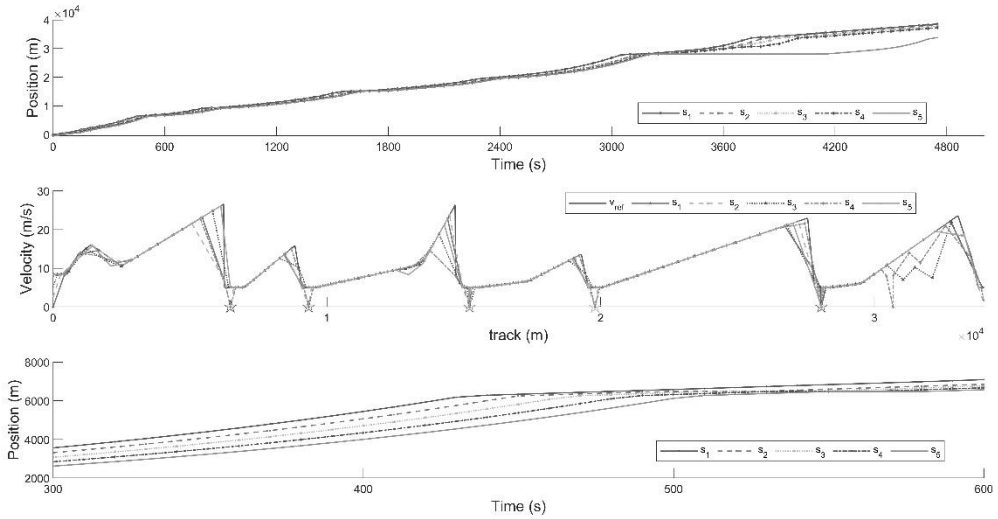


Figure 14. The performance of the virtually coupled trains: a case study of Leeds-Halifax line, UK.